Research paper

In-situ Polymerisation of Fully Bioresorbable Polycaprolactone/Phosphate Glass Fibre Composites: *In Vitro* Degradation and Mechanical Properties

Menghao Chen[1*], Andrew J. Parsons[1], Reda M. Felfel[1, 3], Christopher D. Rudd[1], Derek J. Irvine[2], Ifty Ahmed[1*]

[1]Divison of Materials, Mechanics and Structures, University of Nottingham,
University Park, Nottingham, UK, NG7 2RD

[2]Division of Energy and Sustainability, University of Nottingham
University Park, Nottingham, UK, NG7 2RD

[3]Physics Department, Faculty of Science, Mansoura University, 35516, Egypt

---

ABSTRACT

Fully bioresorbable composites have been investigated in order to replace metal implant plates used for hard tissue repair. Retention of the composite mechanical properties within a physiological environment has been shown to be significantly affected due to loss of the integrity of the fibre/matrix interface. This study investigated phosphate based glass fibre (PGF) reinforced polycaprolactone (PCL) composites with 20%, 35% and 50% fibre volume fractions (V_f) manufactured via an in-situ polymerisation (ISP) process and a conventional laminate stacking (LS) followed by compression moulding. Reinforcing efficiency between the LS and ISP manufacturing process was compared, and the ISP composites revealed significant improvements in mechanical properties when compared to LS composites. The degradation profiles and mechanical properties were monitored in phosphate buffered saline (PBS) at 37°C for 28 days. ISP composites revealed significantly less media uptake and mass loss ($p<0.001$) throughout the degradation period. The initial flexural properties of ISP composites were substantially higher ($p<0.0001$) than those of the LS composites, which showed that the ISP manufacturing process provided a significantly enhanced reinforcement effect than the LS process. During the degradation study, statistically higher flexural property retention profiles were also seen for the ISP composites compared to LS composites. SEM micrographs of fracture surfaces for the LS composites revealed dry fibre bundles and poor fibre dispersion with polymer rich zones, which indicated poor interfacial bonding, distribution and adhesion. In contrast, evenly distributed fibres without dry fibre bundles or polymer rich zones, were clearly observed for the ISP composite samples, which showed that a superior fibre/matrix interface was achieved with highly improved adhesion.

Keywords: biocomposite; bioresorbable; in-situ polymerisation; Poly(ε-caprolactone); phosphate based glass fibres

---

**Corresponding author at:* Division of Materials, Mechanics and Structures, University of Nottingham,
University Park, Nottingham, UK, NG7 2RD.
Tel: +44 (0)1157484675; +44(0)7857816156
Email address: Ifty.ahmed@nottingham.ac.uk; menghaochen88@gmail.com.

Introduction

There is significant scope for improving and developing current load bearing devices for hard tissue repair. The ideal internal bone fixation device should have excellent biocompatibility, be fully bioresorbable, have adequate initial mechanical properties to sustain the mechanical stresses during the surgical procedures and to support bone healing during the initial stages, followed by a gradual decline of its mechanical properties in order to transfer the stress to the healing bone [1, 2]. Fully bioresorbable polymer composites provide a highly attractive opportunity to improve and replace traditional metal implants and are an active research field due to their potential use in load-bearing applications. Biocompatibility of both PCL (approved by FDA) and of phosphate based glass fibre (PGF) has been well investigated and both are known to be bioresorbable, which makes these materials favourable candidates for bone repair applications [3-6]. Most recently, PGF has been used as reinforcement for developing fully bioresorbable polymer composites [2, 7, 8]. PGFs are able to dissolve completely within aqueous media and their dissolution rate can be adjusted easily by altering the glass composition [2]. Fibres with mechanical properties between 500-1200 MPa and 60-80 GPa for tensile strength and modulus respectively, have been achieved which are comparable to commercially available E-glass fibre [8-10]. As an example, PLA/ unidirectional (UD) PGF composites plates with fibre volume fractions (V_f) of 35% and 50% have been produced, which showed flexural strength values of ~116 MPa, ~170 MPa and flexural modulus values of ~16 GPa and ~15 GPa, respectively [11, 12].

Achieving satisfactory adhesion and retention of the fibre and matrix interface has been the main challenge and limitation in matching the degradation rate of the composites with bone healing process. The most frequently used manufacturing technique adapted for bioresorbable polymer composites is laminate stacking (LS) and hot press moulding [13-15]. However, a number of studies have seen a rapid loss in mechanical properties of the composites manufactured by LS after immersion in aqueous environment [2, 12, 16, 17]. It is believed that rapid hydrolysis of the polymer/fibre interfaces happened, which reduced adhesion and prevented efficient stress transfer between matrix and reinforcement. Due to the high viscosity of the polymer melt, it is difficult to gain a good impregnation and wet-out of the fibre surface by using the LS technique, which often result in poor fibre/matrix adhesion. Poor interfacial bonding is more vulnerable to fluid ingress through the interfaces under aqueous environments, which leads to a rapid loss of mechanical properties and early stage failure of the composites [18]. As such, it is of paramount importance for bioresorbable fibre reinforced composites to achieve strong fibre/matrix adhesion in order for their successful application in the field of hard tissue repair. In addition, since the fibre mats and polymer films are stacked together, the composites produced tend to form polymer rich zones and fail via delamination [12, 17]. The secondary melting process of the polymers can also cause thermal degradation of the matrix material.

In this study, in-situ polymerisation (a variant of liquid moulding based on the monomer transfer moulding (MTM) technique) was developed and investigated to manufacture fully bioresorbable PCL/PGF composites. Similar approaches such as Resin Transfer Moulding (RTM) and Structural Resin Injection Moulding (SRIM) in the thermoset composites manufacturing are well established. However, the counterpart in the thermoplastic composites manufacturing is rarely reported. Instead of using resin, a reaction mixture (monomer and catalyst) was injected into moulds and polymerised in situ to form the matrix directly around the reinforcement within a single step. Since the viscosity of the monomer (ε-caprolactone at room temperature: 1.07 mPa s) is much lower in comparison to the polymer melt (PCL melt: 12,650 Pa s), good fibre impregnation and significantly enhanced interfacial bonding could be obtained by ISP [16]. This should lead to higher mechanical properties and a better degradation profile for the biodegradable implants. This technique allows direct control on molecular weight of the polymer matrix by altering the amount of initiator in the system. Composite implants with complicated shapes can also be produced by ISP as closed moulds with complex cavity shapes can be manufactured. Corden *et.al* [19, 20] investigated the physical and biocompatibility properties of PCL

produced via ISP and reported a good biocompatibility. They also produced PCL/woven and knitted vicryl mesh composites via ISP and SEM micrographs showed that the fibres were fully impregnated with PCL [19]. Jiang *et al.* [21] also produced bioresorbable PCL/Bioglass fibre composites using ISP and recorded their degradation profiles in double distilled water (DDW) up to 7 weeks. The composites with 25% V_f had initial flexural modulus and strength values of 16 GPa and 200 MPa respectively, while after 21 days of degradation they reduced to ~7 GPa and ~65 MPa respectively [21].

Fully bioresorbable PCL/PGF composites with V_f of 20%, 35% and 50% were manufactured via both LS and ISP in order to compare between the reinforcing efficiency of both manufacturing processes. A degradation study was performed on the composites in Phosphate Buffered Saline (PBS) up to 4 weeks at 37 °C, in which their mechanical property retention, pH, media up-take and weight loss were monitored. Change in molecular weight and distribution were also determined via Gel Permeation Chromatography (GPC) and SEM micrographs revealed the fibre distribution and fibre/matrix interface.

Materials and Methods

Materials

The monomer ε-caprolactone, catalyst $Sn(Oct)_2$ and initiator benzyl alcohol were all purchased from Sigma Aldrich (UK), with purities reported as 97%, 92.5%~100% and 99.8% respectively. As the polymerisation is highly sensitive to moisture, the chemical mixture was degassed via a freeze-pump-thaw technique for 3 cycles in order to remove any excess water in the system just before use. PCL granules used were purchased from Sigma Aldrich (UK) and reported to have a weight average molecular weight (M_w) of ~65,000 g/mol and number average molecular weight (M_n) of ~42,500 g/mol. The granules were dried at 50 °C in a vacuum oven for 48 hours before processing.

Polymerisation chemistry

PCL can be synthesised from both condensation polymerisation (CP) and ring opening polymerisation (ROP). Due to the difficulty in removing the water during CP, ROP is usually used in order to yield high molecular weight polymers.

In this study, coordination insertion polymerisation mechanism (CIM) was chosen with $Sn(Oct)_2$ used as the pre-catalyst and benzyl alcohol as the initiator. CIM is known to be selective and can significantly suppress undesired side reactions such as inter- and intra-molecular transesterifications that makes close control of the molecular weight and polydispersity (PDI) became feasible [22]. The reaction mechanism is illustrated in Figure 1. $Sn(Oct)_2$ initially reacts with benzyl alcohol to form the active catalyst species for PCL ROP. The monomer then coordinates with the catalyst, which induces strain in the monomer ring. The monomer is finally inserted into the Sn-O bond by acyl-oxygen bond scission so that the growing chain remains attached to tin through an alkoxide bond. The CIM method generally results in well-defined polymers with high molecular weight and narrow polydispersity.

Phosphate glass and glass fibre mats production

Bioresorbable phosphate based glass was produced in order to manufacture phosphate glass fibres. The precursors used to prepare the glass were sodium hydrogen phosphate (NaH_2PO_4), calcium hydrogen phosphate ($CaHPO_4$), magnesium hydrogen phosphate tri-hydrate ($MgHPO_4 \cdot 3H_2O$), iron(III) phosphate di-hydrate ($FePO_4 \cdot 2H_2O$) and phosphorous pentoxide (P_2O_5), which were all purchased from Sigma Aldrich

(UK). The glass formulation used in this study (with its respective glass code) is reported in Table 1. The precursors were mixed together and then transferred into a 100 ml Pt/5% Au crucible (Birmingham Metal Company, UK). The crucible was then placed in a preheated oven (350 °C) for 30 minutes to remove any water within the mixture. The salt mixtures were then melted and reacted at 1150 °C for 1.5 hours in a furnace. Molten glass was poured onto a steel plate to cool down.

The in-house designed fibre rig consists of a furnace (Lenton Furnaces, UK) with a Pt/10% Rh crucible (Johnson Matthey, UK) consisting of a bushing with an approximate 1 mm hole and a tip 15 mm long. Glass was placed into the crucible and left to melt and homogenise for 30 minutes. The temperature of the furnace was then decreased to achieve a viscosity suitable for fibre drawing. Different fibre diameters can be obtained by pulling the glass at different speeds. In order to produce the unidirectional fibre mats, the collecting drum was adjusted to move transversely at constant speed, covering the drum evenly with fibre. After the fibre mat had reached a certain thickness, the fibre drawing was stopped and the drum was taken to a fume hood. To maintain the integrity of the fibre mat alignment, a solution of PCL dissolved in chloroform (5% concentration) was sprayed onto the fibre mat to coat them. Afterwards, the drum was left inside the fume hood for 24 hours to let the chloroform evaporate. Finally, the coated fibre mat was removed from the drum and PGFs were produced of parallel filaments without any twist.

PGF/PCL composites production

PCL/PGF composites with three different fibre volume fractions were produced via both LS and ISP manufacturing techniques. Details of the composites produced are listed in Table 2.

Laminate stacking (LS) technique

Thin sheets PCL (thickness ~0.2 mm) were prepared by hot press moulding of 4~5 g PCL granules. The granules were placed between metal plates, with PTFE coated glass fabric sheets used as release film. The whole assembly and granules were heated to 120 °C within the hot press for 10 minutes and then pressed at 3 bar for 1 minute. The assembly was then transferred to a cold press at room temperature to cool down under the same pressure.

All PCL films and fibre mats were dried in a 50 °C vacuum oven for 24 hours prior to use. The PCL/PGF laminates were prepared by film stacking technique. Both PCL laminates and PGFs were cut to fit the mould cavity. The assembly was then heated to 120 °C within the hot press for 15 minutes, pressed under 30 bar for 10 minutes. The stack was then transferred immediately to a cold press at room temperature to cool down under the same pressure for 15 minutes. The composite plate was then removed from the mould and cut into dimensions of 40mm × 15mm × 2mm using a band saw for sample testing.

In-situ polymerisation (ISP) technique

ISP Mould design

In order to perform ISP of PCL/PGF composites, moulds were designed and made using PTFE and aluminium (see Fig.2). PTFE was chosen as the material as it is chemically inert, thermally stable and beneficial for sample de-moulding. Each mould consisted of a female and male half PTFE block, and two aluminium blocks, which acted as the outer shells to protect the PTFE moulds. The aluminium blocks also helped to flatten the PTFE moulds as PTFE is prone to distortion under stress and heating. The mould halves were assembled using long screws and nuts. Two injection ports were located on the male half, one for liquid

injection and the other for degassing. The sample cavity was positioned on the female half and surrounded by an O-ring cord groove to provide a tight sealing. O-rings were also incorporated around the injection ports.

ISP manufacturing process

The mould assembly used for ISP and the mixing and injection apparatus were all dried at 50 °C for 24 hours in a vacuum oven before processing. UD PGF mats were carefully trimmed to fit the cavity of the mould (70mm×15mm×2mm and 130mm×165mm×2mm). The trimmed fibre mats were also dried under the same conditions as the moulds. Monomer ε-caprolactone was treated with a predetermined amount of $Sn(Oct)_2$ and benzyl alcohol under a dry nitrogen atmosphere using a 100 ml two neck boiling flask. The reaction solution was mixed using a magnetic stirrer until homogeneous. After the mixing was completed, it was then injected into the moulds using a syringe. Each injection port was connected with one syringe by PTFE tubing, one with the chemical mixture and one empty. The reaction mixture was injected backwards and forwards from one syringe to the other in order to eliminate air bubbles in the moulds and to ensure a smooth injection process. After the injection process was completed, two tubing clamps were used to seal the tubing and the syringes were removed. Consequently, the mould assembly was transferred to a preheated oven for 24 hours to complete the polymerisation reaction. Finally, moulds were disassembled and samples were taken out of the moulds.

Degradation study

The degradation study was performed according to the standard BS EN ISO 10993-13. PCL/PGF composites and PCL plates were cut into specimens with dimensions of 40mm × 15mm × 2mm. The weight of each specimen was recorded before placing them into 30 ml glass vials individually. 30 ml of PBS (pH=7.4 ± 0.2) was added to each vial to fully immerse the specimen. Vials were kept at 37 °C for 28 days. At various time points (0, 1, 3, 7, 11, 15, 21 and 28 days), specimens were extracted and blot dried before measuring the wet weight. pH of the degradation media was also monitored at each time point using a bench-top pH meter (pH 212, Hanna Instruments, UK). The solution was replaced by fresh PBS solution at each time point. The extracted specimens were dried at 50 °C for 48 hours in order to evaluate their mass loss. The specimen mass loss (M_d) and media uptake (W) were calculated using the following equations:

$$M_d = \frac{m_d - m_i}{m_i} \times 100\%$$

$$W = \frac{m - m_d}{m_d} \times 100\%$$

where m is the mass of the blot dried specimen at each time point, m_i is the initial dry mass and m_d is the mass of degraded sample after drying at 50 °C for 48 hours.

Flexural tests

Flexural strength and modulus were determined via 3 point bending tests using a Bose ElectroForce® Series II 3330. Both non-degraded and degraded composites specimens were measured to monitor the change in mechanical properties over the degradation time. Tests were performed according to standard BS EN ISO 14125:1998. Specimen dimensions of 40mm × 15mm × 2mm, a cross-head speed of 1 mm/min and a 1 kN load cell were used. Tests were performed in triplicate (n=3).

Scanning Electron Microscopy (SEM)

SEM was performed to analyse the polymer/fibre interface and fibre distribution at freeze-fracture surfaces for both LS and ISP samples. Secondary electron mode was used with a voltage of 10 keV. Composite samples were all sputter-coated with platinum prior to testing.

Gel Permeation Chromatography (GPC)

GPC was performed to analyse the molecular weight and molecular weight distribution. The GPC used was an Agilent Technologies 1260 Infinity GPC system with mixed D columns at 40 °C and a refractive index detector. Chloroform was used as the mobile phase at a flow rate of 1.0 cm^3/min. Calibration was accomplished against PMMA standards. The calibration range of the GPC was from 10 min to 17.35 min elution time, corresponding to molecular weights from 580 g/mol to 377,400 g/mol. Sample concentration was ca. 5 mg/ml.

Burn off test

Burn-off tests were performed on all composites samples in order to determine the actual fibre volume fraction. Tests were performed according to standard BS EN ISO 2782-10. The results are presented in Table 2 (n=5).

Single fibre tensile test

Tensile modulus and strength of the fibres were measured using a single fibre tensile tester (Diastron LEX-810 Tensile tester with attached Mitutoyo series 544 LSM-500S laser diameter monitor). The test was performed according to the standard BS ISO11566. 30 fibres were tested with a gauge length of 25mm (n = 30).

Rule of mixture

Theoretical Young's modulus of fibre reinforced composites can be predicted using the following equation:

$$E = \eta_L \eta_o E_f V_f + E_m (1 - V_f)$$

where η_L and η_o represent fibre length correction and orientation efficiency factors. For unidirectional fibre composites, both η_L and η_o equal 1. E_f and E_m are Young's modulus for the fibres and polymer matrix. Young's modulus of unidirectional fibre reinforced composites can be predicted by using properties of fibre and matrix along with fibre volume fraction data (See Table 2).

Statistical analysis

Data were presented graphically as mean ± standard deviation. Measured data were analysed by Microsoft Excel using a student's unpaired t-test, assuming equal variance with Microsoft Excel. Statistical significance ranking was defined as $p>0.05$ (statistically insignificant), $p<0.05$ (statistically significant), $p<0.01$ (very statistically significant) and $p<0.0001$ (extremely statistically significant).

Results

Media uptake

Figures 3a and 3b shows the change in percentage of media uptake versus time for PCL and PCL/PGF composites manufactured via LS and ISP processes during degradation in PBS at 37 °C for 28 days. Both LSPCL and ISPPCL maintained a constant media uptake (~0.5%) throughout the 28 days of immersion. By comparing the media uptake profiles for LS20, LS35 and LS50, it was seen that amounts of media uptake increased by increasing fibre volume fraction over the same immersion time (similar trend was observed for ISP20, ISP35 and ISP50).

By comparing Figure 3a and 3b, the media uptake profiles of the LS and ISP PCL/PGF composites with the same fibre volume fractions exhibited very similar trends. An approximately linear increase was observed up to 21 days of immersion followed by a reduction in the rate of media uptake till the end of the study. However, in absolute terms, significantly higher amounts of media was absorbed ($p<0.05$) by the LS composites in comparison to the ISP composites at all time-points. The LS20, LS35 and LS50 composites absorbed approximately 43%, 44% and 42% more media than their respective ISP equivalents at day 28.

Mass loss

Figure 3a and 3b also show the percentage of mass loss against degradation time for PCL and PCL/PGF composites manufactured via LS and ISP. Both neat LSPCL and ISPPCL showed no significant mass loss throughout the degradation period. Similar profiles of mass loss curves between LS and ISP composites were observed, in which an initial mass loss after 1 day immersion (~0.2%) was recorded, followed by a linear increase up to the end of the study (28 days). By comparing LS and ISP composites with the same V_f, it can be seen that LS composites showed a significantly higher mass loss ($p<0.001$) than the ISP composites. At the end of the degradation study (28 days), LS composites with V_f of 20%, 35% and 50% had lost approximately 41%, 42% and 35% more mass than their respective ISP composites.

pH change

The variation of pH values of the PBS solution for PCL and PCL/PGF composites manufactured via LS and ISP are presented in Figure 4a and 4b respectively. The pH for LSPCL and ISPPCL remained neutral at 7.4 ± 0.2 till the end of the degradation study. However, the pH profiles for all composites remained stable at 7.4 ± 0.2 until the 11 day interval, after which a gradual decrease was observed up to 28 days. At the same V_f, LS composites showed significantly larger pH drop ($p<0.05$) than ISP composites between 11 and 28 days of immersion.

Molecular weight and distribution

Change in molecular weight (M_w) against degradation for PCL and PCL/PGF composites produced by LS and ISP are shown in Figure 5a. There was no significant difference ($p>0.05$) seen in M_w between non-degraded neat LSPCL and LS composites. The values of M_w for LSPCL and LS20 did not show any significant change ($p>0.05$), whilst both LS35 and LS50 gradually decreased by ~7% by the 28 day interval, where the drop in M_w was found to be statistically significant ($p<0.05$). Similarly, the M_w of ISPPCL remained stable for the 28 day study, while the M_w of ISP20, ISP35 and ISP50 gradually decreased by ~6%, ~10% and ~7% respectively ($p<0.05$). Moreover, only the non-degraded ISPPCL exhibited a similar M_w to the LSPCL and LS composites

(~90,000 g/mol), which was considerably higher ($P<0.0001$) than the M_w of the ISP composites (~45,000 g/mol for ISP20, ISP35 and ISP50). Figure 5b exhibited the polydispersity index (PDI) data of all the LS and ISP specimens over 28 days of immersion. It can be seen that the PDI of all specimens was similar (1.2~1.4) and no significant variation ($p>0.05$) was observed over the whole period of study. However, it was noticed that the PDI of ISPPCL (~1.2) stayed slightly lower than all other composites over the 28 day period.

Flexural Properties

Figures 6a and 6b show that the flexural strength and modulus decreased with immersion time for all PCL/PGF composites. However, both LSPCL and ISPPCL maintained their flexural strength and modulus for the whole degradation period, with no statistically significant difference found between the flexural properties of the LSPCL and ISPPCL specimens ($p>0.05$).

By comparing the initial (non-degraded) flexural strength and modulus values between LS and ISP composites with the same V_f, it can be seen that ISP composites had significantly higher ($p<0.001$) flexural properties than LS composites, with increases of ~11%, ~30% and ~42% in flexural strength and ~28%, ~36% and 37% in modulus observed for ISP20, ISP35 and ISP50 composites respectively. It was also noticed that ISP35 (V_f=35%) had significantly higher ($p<0.05$) flexural strength and modulus than the ISP50 (V_f=50%) composites. Similar profiles of flexural properties were obtained for all LS and ISP composites, a sharp decrease after 1 day immersion in PBS followed by a plateau until day 11 for modulus and day 15 for strength, after which a further drop was seen until the end of study. Furthermore, the flexural properties of ISP composites remained statistically higher than all LS composites after 28 days of degradation.

The flexural strength for all LS composites was significantly lower ($p<0.05$) than LSPCL after 21 days of immersion, whilst all ISP composites maintained a higher strength than ISPPCL. However, it was also noted that after 28 days of immersion, only ISP20 exhibited higher flexural strength than pure PCL, whilst all other composites showed significantly lower ($P<0.05$) flexural strength than pure PCL. In addition, all composites (LS and ISP) maintained a significantly higher ($P>0.05$) flexural modulus than pure PCL until the end of the study (28 days).

SEM analysis

Figure 7 shows the SEM micrographs of freeze fractured and cut polished surfaces of non-degraded LS35 and ISP35 composites. SEM micrographs of composites with 20% and 50% V_f were very similar (data not shown). The LS35 and ISP35 composites were selected to represent and illustrate the reinforcing effect of the LS and ISP composites that were produced. From Figure 7a and 7c, the individual layers of PCL and UD PGF mats can be seen clearly, with polymer rich zones between the fibre layers and extensive areas of dry fibre within the fibre layers. In contrast, uniform fibre distributions were observed in Figure 7b and 7d throughout the entire cross sectional area of the ISP35 composites. No obvious polymer rich zones or dry fibres were detected in the composites manufactured via the ISP process.

SEM micrographs of freeze fractured surfaces for LS35 and ISP35 composites at selected degradation time points (1, 15 and 28 days of degradation) are presented in Figure 8. Different phenomena can be seen from the micrographs: micro tubes resulting from fibre degradation (Figure 8c and 8f), fibre pull out sites in LS35 composites (Figure 8a and 8b) and fibre fracture with no pull out in ISP35 composites (Figure 8d and 8e).

Discussions

In this study, fully bioresorbable PGF reinforced PCL composites were produced via both LS and in-situ polymerised (ISP) manufacturing processes. The aim of this study was to develop the ISP process for bioresorbable composite manufacturing and investigate the reinforcing efficiency in comparison to conventional LS processes. Jiang *et al.* [21] reported that the ISP process could significantly enhance the fibre/matrix adhesion and interfacial bonding for PCL/continuous bioglass fibre composites, which indicated its potential in improving the degradation profile of PCL/PGF composites.

The formation of extensive dry fibre bundles and polymer rich zones in LS composites were resulted from the high viscosity of the polymer melt during the LS process (see Figure 7a and 7c). This meant that the polymer melt only had limited flow under pressure, making it very difficult to achieve sufficient wet-out and impregnation around and within fibre mats. As such, the presence of these dry fibre bundles led to lack of interfacial bonding, which only provided limited reinforcement and transfer of stress within these composites. As such, the mechanical properties of the composites were significantly below expectation due to the poor efficiency of fibre reinforcement. These composites also tend to fail via delamination at the early stages of load-bearing due to the lack of reinforcement within the polymer rich zones [13, 23].

In contrast, SEM micrographs of the non-degraded ISP35 composites (see Figures 7b and 7d) suggested that a more robust fibre/matrix interfacial bonding and even fibre distribution had successfully been achieved via the ISP process as no noticeable dry fibre bundles and polymer rich zones were observed. The viscosity of the monomer was significantly lower than the polymer melt, which allowed improved flow properties within and between the fibre bundles, thus resulted in significantly enhancing the fibre wet-out and impregnation [20, 21]. Furthermore, the direct polymerisation also allowed for a one-step net shape production of composites, whereas making polymer films was the pre-requisite for the LS process. The enhanced fibre reinforcement also correlated well with the results from rule of mixtures. It can be seen in Table 3 that the theoretical and experimental values of flexural modulus were very similar for the ISP composites, whilst the theoretical flexural modulus for the LS composites were significantly lower ($P<0.001$) than the experimental data. This suggested that robust interfacial bonding via the ISP process with complete fibre impregnation had been achieved (see Figure 7b and 7d).

In addition, Figure 9 showed that the strain at failure of LS20 ($\varepsilon = \sim 1.05\%$) was significantly lower than that of ISP20 ($\varepsilon = \sim 1.55\%$), which indicated early failure of LS composites due to poor interfacial bonding (LS35 and LS50 exhibited a similar trend, data not shown here). The profile of the stress strain curves also indicated very different failure mechanisms for the composites. The LS composites showed a more ductile failure mechanism, suggesting progressive fibre pull out had occurred. Whilst, a brittle failure mode was observed for the ISP composites and the stress was seen to increase linearly until composite failure. Higher failure stress was also observed for the ISP composites. The difference in failure mechanisms also correlated well with the SEM micrographs of the fracture surfaces, where fibre pull-out were observed for the LS composites and clean fibre breakages for the ISP composites (see Figure 7 and 8).

The media uptake of composites is usually higher than for the polymer alone, since the media is more prone to diffusion along the fibre/matrix interfaces by capillary action (See Figure 3a and 3b). The fibres within the composite samples were exposed at the edges and hence the fibre/matrix interfaces were directly exposed to the aqueous environment during immersion, where wicking effects could occur and are known to be responsible for the increase of media uptake in the composites [24]. It was also seen that the amount of media absorbed by composites increased with higher V_f, which was as ascribed to the increase in the amount of interfacial area with increasing V_f. When comparing the media uptake profiles of the LS composites with ISP

composites at the same V_f, it was seen that ISP composites absorbed significantly less media than LS composites ($p<0.05$). This correlated well with the stronger interfacial bonding promoted by ISP process compared to the LS process, in which there were less voids or channels for media to pass through. Additionally, the rapid increase in media uptake was attributed to fibre degradation itself, clear evidence for fibre degradation was seen at later time points (See Figure 8c and 8f). The media uptake profiles for all composites exhibited a tendency to decrease after day 21, which indicated that the media was getting saturated within the composites and most, if not all, of the fibre/matrix interfaces had been degraded, followed by a reduction in degradation of the fibres.

For both LS and ISP composites, increasing V_f resulted in an increasing amount of mass loss within the same degradation time (see Figure 3a and 3b). This was suggested to be due to the larger amount of fibres within the composites, which also increased the contact surface areas between fibre and PBS, hence more fibre degradation occurred. For LS and ISP composites with the same V_f, significantly less mass loss was seen for ISP composites ($p<0.001$), which indicated that the ISP composites were more resistant to PBS degradation than LS composites. The stronger interface of ISP composites protected more PGF fibres from contacting PBS, thus less fibre degradation, which correlated well with media uptake profile as less media was absorbed by ISP composites. Ahmed *et al.* [25] investigated the degradation behaviour of a binary calcium phosphate-based glass fibre reinforced PCL composites (V_f = ~6% and ~14%) within deionized water at 37°C for up to 900 hours. They reported similar mass loss profiles that exhibited a linear mass degradation up to 250 hours.

From Figure 4, the reduction of pH for both LS and ISP composites started from day 11, whilst the mass loss was shown to be linear with degradation time. This would suggest that there is a delayed loss of acidic materials that could be due to the buffering effect of PBS and progressive dissolution of fibre. The resulting acidity was attributed to phosphate ions from the fibres being released from the composite into solution, forming H_3PO_4 (phosphoric acid) [12]. The relatively higher pH of the ISP composites compared to the LS composites suggested that less degradation has occurred, hence the slower fibre degradation rate for the ISP composites. This is supported by the mass loss data as well. The pH started to drop faster from day 21, which suggested major fibre degradation, and leaving behind micro tubes within the composites at the end of the study (See Figure 8c and 8f).

Both neat LSPCL and ISPPCL did not show any reduction in molecular weight over 28 days of immersion. However, all the PGF/PCL composites manufactured via LS and ISP exhibited significant decrease ($p<0.05$) in molecular weight after 28 days of immersion (see Figure 5a). Degradation of PCL within PBS often occurs through hydrolysis and chain scission. This indicated that the inclusion of PGFs accelerated the hydrolytic degradation of PCL as a result of the acidic breakdown products from PGF glass fibre catalysing the hydrolysis process. Similar molecular weight variations were observed by Haltia *et al.*[26]. They monitored the hydrolytic degradation of self-reinforced poly(ester-amide) rods within PBS at 37°C. They reported that degradation at the fibre/matrix interfaces was faster than in the matrix and the diffusion of PBS through the fibre/matrix interfaces accelerated the degradation of the matrix by hydrolysis.

All the specimens manufactured via LS exhibited an initial (non-degraded) molecular weight of ~90,000 g/mol (see Figure 5a), while only ISPPCL showed a similar initial molecular weight. The ISP20, ISP35 and ISP50 exhibited approximately half the targeted molecular weight (~45,000 g/mol). The in-situ polymerisation of all PCL and PCL/PGF composite specimens were performed with the same reaction parameters. The large decrease in molecular weight was attributed to excess moisture content in the reaction system presumably introduced via the PGF mats. Kinetic studies of PCL polymerisation [27] found that the reaction system was highly sensitive to moisture, where excess water in the reaction system could act as a competitive initiator for the ε-caprolactone polymerisation since both water and benzyl alcohol molecules have active hydroxyl

groups. PGF mats were dried in the 50°C vacuum oven 48 hours prior to use in order to remove any excess moisture. However, it is suspected that some moisture content remained on the PGFs which caused the decrease in molecular weight of the polymer in the ISP composites. In addition, the PGF mats were bound together using a PCL coating solution, for which the PCL utilised had a specified molecular weight. It is also suggested that the PCL binding solution used could have been degraded under heating via the ISP process, and the degradation products could have hindered the ISP reaction. However, further studies are required to confirm the cause of the low molecular weight synthesised via the in-situ polymerisation process.

The flexural strength and modulus of all PCL/PGF composite specimens in this study exhibited an initial reduction after immersion in PBS for 1 day, which was suggested to be due to plasticisation of the fibre/matrix interface by the diffused PBS within the composite specimens [14, 16, 28]. The diffused PBS might also cause micro cracks and stress concentration sites on the fibre surfaces and led to the reduction in composites mechanical properties [2]. A further decrease in the flexural properties was observed after 11 to 15 days of immersion, which was attributed to the partial degradation of PCL and PGFs themselves and the degradation of the fibre/matrix interfaces. This is well supported by the pH profiles as they indicated significant fibre degradation occurred from day 11 to day 15. The degradation profile of PLLA composites with different types of fibres within PBS were studied by Slivka *et al.* [24]. They reported that an increasing interfacial gap was seen during 30 days of immersion using a laser confocal microscope, which confirmed that interface degradation had occurred during the study. Lin *et al.* [29] also found a similar reduction in mechanical properties for calcium phosphate glass fibre reinforced PLLA composites (V_f = ~55%). They found that the initial flexural strength and modulus as ~350 MPa and ~28 GPa, which decreased to ~84 MPa and ~3.8 GPa respectively after 1 week of immersion in PBS at 37°C. They stated that the observed decrease was ascribed to the breakdown of the fibre/matrix interface and fibre degradation.

From Figure 6a and 6b, the initial flexural strength and modulus values for all ISP composites were statistically higher than the LS composites at all time points throughout the study. All the composites exhibited properties which were within the range of the flexural properties of cortical bones (E = 5-23 GPa, σ = 35-280 MPa) [30, 31]. It is well known that the strength of the fibre/matrix interface is critical to the mechanical properties of fibre reinforced composites [9, 32-34]. Although the molecular weight of the ISP composites was much lower than that of LS composites, the flexural properties of the ISP composites were still significantly higher, which proved that ISP process delivered a significantly enhanced interfacial bonding and adhesion. It was also noted that both the flexural strength and modulus of the non-degraded ISP35 were even higher ($p<0.001$) than LS50 composites. This also suggests that if the ISP process can yield higher molecular weight of the PCL matrix then further enhancements of the mechanical properties could be achieved. Furthermore, it was seen that only ISP20 had higher flexural strength than pure PCL after 28 days degradation (see Figure 6a) that indicated that fibre reinforcements were no longer contributing to the mechanical properties of all the other composites. The degradation of the fibres was effectively developing pores/channels inside the matrix, which could also enhance the PCL matrix degradation. In summary, the PGF/PCL composites manufactured via ISP process revealed superior mechanical properties, degradation profiles and mechanical property retention in comparison to those manufactured via the LS process.

Conclusions

SEM micrographs of fractured cross sections of the LS composites revealed dry fibre bundles and poor fibre dispersion with extensive polymer rich zones. Conversely, even fibre distributions with no dry fibre bundles or polymer rich zones were observed for the ISP composites. Via the ISP manufacturing process, the bioresorbable PCL/PGF composites also had significantly prolonged and higher retention of mechanical properties over the 28 day degradation study within PBS at 37 °C. These differences showed that a robust and significantly stronger fibre/matrix interface had been achieved via the ISP process.

An enhanced fibre/matrix interface resulted in a significant decrease of voids or channels within the composites, leading to reduced degradation rate for all the ISP composites. This correlated well with the media uptake and mass loss profiles, which showed that the ISP composites had significantly lower levels of media absorption and mass loss ($p<0.001$ for both data) during the degradation period. Molecular weight and distribution did not show any significant variation for pure PCL over 28 days, while significant decrease ($p<0.05$) was noted for all PCL/PGF composites. The accelerated degradation of the matrix was attributed to the acidic breakdown products from fibre degradation, which could have catalysed matrix hydrolysis. Overall the ISP process showed significant improvements over the LS process in manufacturing fully bioresorbable composites.

Acknowledgments

The author would like to acknowledge the University of Nottingham for awarding this studentship through the Dean of Engineering Research Scholarship for International Excellence.

References

1. Huttunen, M., et al., *Fiber-reinforced bioactive and bioabsorbable hybrid composites.* Biomedical Materials, 2008. **3**(3).
2. Parsons, A.J., et al., *Phosphate Glass Fibre Composites for Bone Repair.* Journal of Bionic Engineering, 2009. **6**(4): p. 318-323.
3. Sun, H., et al., *The in vivo degradation, absorption and excretion of PCL-based implant.* Biomaterials, 2006. **27**(9): p. 1735-1740.
4. Salih, V., et al., *Development of soluble glasses for biomedical use Part II: The biological response of human osteoblast cell lines to phosphate-based soluble glasses.* Journal of Materials Science: Materials in Medicine, 2000. **11**(10): p. 615-620.
5. Manhart, J., et al., *Mechanical properties of new composite restorative materials.* Journal of Biomedical Materials Research, 2000. **53**(4): p. 353-361.
6. Li, S. and M. Vert, *Biodegradation of Aliphatic Polyesters*, in *Degradable Polymers*, G. Scott, Editor. 2002, Springer Netherlands. p. 71-131.
7. Mohammadi, M.S., et al., *Effect of phosphate-based glass fibre surface properties on thermally produced poly(lactic acid) matrix composites.* J Mater Sci Mater Med, 2011. **22**(12): p. 2659-72.
8. Ahmed, I., et al., *Processing, characterisation and biocompatibility of iron-phosphate glass fibres for tissue engineering.* Biomaterials, 2004. **25**(16): p. 3223-3232.
9. Haque, P., et al., *Influence of compatibilizing agent molecular structure on the mechanical properties of phosphate glass fiber-reinforced PLA composites.* Journal of Polymer Science Part A: Polymer Chemistry, 2010. **48**(14): p. 3082-3094.

10. Sharmin, N., et al., *Effect of boron oxide addition on fibre drawing, mechanical properties and dissolution behaviour of phosphate-based glass fibres with fixed 40, 45 and 50 mol% P2O5.* Journal of Biomaterials Applications, 2014. **29**(5): p. 639-653.
11. Brauer, D., et al., *Degradable phosphate glass fiber reinforced polymer matrices: mechanical properties and cell response.* Journal of Materials Science: Materials in Medicine, 2008. **19**(1): p. 121-127.
12. Ahmed, I., et al., *Retention of mechanical properties and cytocompatibility of a phosphate-based glass fiber/polylactic acid composite.* Journal of Biomedical Materials Research Part B: Applied Biomaterials, 2009. **89B**(1): p. 18-27.
13. Ramakrishna, S., et al., *Biomedical applications of polymer-composite materials: a review.* Composites Science and Technology, 2001. **61**(9): p. 1189-1224.
14. Imai, Y., M. Nagai, and M. Watanabe, *Degradation of composite materials composed of tricalcium phosphate and a new type of block polyester containing a poly(L-lactic acid) segment.* Journal of Biomaterials Science, Polymer Edition, 1999. **10**(4): p. 421-432.
15. Mano, J.F., et al., *Bioinert, biodegradable and injectable polymeric matrix composites for hard tissue replacement: state of the art and recent developments.* Composites Science and Technology, 2004. **64**(6): p. 789-817.
16. Felfel, R.M., et al., *In vitro degradation, flexural, compressive and shear properties of fully bioresorbable composite rods.* Journal of the Mechanical Behavior of Biomedical Materials, 2011. **4**(7): p. 1462-1472.
17. Parsons, A., et al., *Mechanical and degradation properties of phosphate based glass fibre/PLA composites with different fibre treatment regimes.* Science and Engineering of Composite Materials, 2010. **17**(4): p. 243-260.
18. Furukawa, T., et al., *Biodegradation behavior of ultra-high-strength hydroxyapatite/poly (l-lactide) composite rods for internal fixation of bone fractures.* Biomaterials, 2000. **21**(9): p. 889-898.
19. Christian, P., et al., *Monomer transfer moulding and rapid prototyping methods for fibre reinforced thermoplastics for medical applications.* Composites Part A: Applied Science and Manufacturing, 2001. **32**(7): p. 969-976.
20. Corden, T.J., et al., *Initial development into a novel technique for manufacturing a long fibre thermoplastic bioabsorbable composite: in-situ polymerisation of poly-ϵ-caprolactone.* Composites Part A: Applied Science and Manufacturing, 1999. **30**(6): p. 737-746.
21. Jiang, G., et al., *Preparation of poly(ε-caprolactone)/continuous bioglass fibre composite using monomer transfer moulding for bone implant.* Biomaterials, 2005. **26**(15): p. 2281-2288.
22. Kricheldorf, H.R. and D.-O. Damrau, *Polylactones, 42. Zn L-lactate-catalyzed polymerizations of 1,4-dioxan-2-one.* Macromolecular Chemistry and Physics, 1998. **199**(6): p. 1089-1097.
23. Edwards, K.L., *An overview of the technology of fibre-reinforced plastics for design purposes.* Materials & Design, 1998. **19**(1–2): p. 1-10.
24. Slivka, M.A., C.C. Chu, and I.A. Adisaputro, *Fiber-matrix interface studies on bioabsorbable composite materials for internal fixation of bone fractures. I. Raw material evaluation and measurement of fiber—matrix interfacial adhesion.* Journal of Biomedical Materials Research, 1997. **36**(4): p. 469-477.
25. Ahmed, I., et al., *Weight loss, ion release and initial mechanical properties of a binary calcium phosphate glass fibre/PCL composite.* Acta Biomaterialia, 2008. **4**(5): p. 1307-1314.
26. Haltia, A.-M., et al., *Self-reinforcement and hydrolytic degradation of amorphous lactic acid based poly(ester-amide), and of its composite with sol-gel derived fibers.* Journal of Materials Science: Materials in Medicine, 2002. **13**(10): p. 903-909.

27. Chen, M., et al., *Developing an in-situ polymerisation process for biocomposite manufacturing*, in *20th International Conference on Composite Materials*. 2015, ICCM20 Organizing Committee: Copenhagen.
28. Liu, X., et al., *Mechanical, degradation and cytocompatibility properties of magnesium coated phosphate glass fibre reinforced polycaprolactone composites.* Journal of Biomaterials Applications, 2014. **29**(5): p. 675-687.
29. Lin, S.T., et al., *Development of bioabsorbable glass fibres.* Biomaterials, 1994. **15**(13): p. 1057-1061.
30. Fung, Y.-C., *Biomechanics: mechanical properties of living tissues*. 2013: Springer Science & Business Media.
31. Wang, X., et al., *The role of collagen in determining bone mechanical properties.* Journal of Orthopaedic Research, 2001. **19**(6): p. 1021-1026.
32. Thomason, J.L. and L. Yang, *Temperature dependence of the interfacial shear strength in glass-fibre epoxy composites.* Composites Science and Technology, 2014. **96**: p. 7-12.
33. Yang, L. and J.L. Thomason, *Effect of silane coupling agent on mechanical performance of glass fibre.* Journal of Materials Science, 2013. **48**(5): p. 1947-1954.
34. Yang, L. and J.L. Thomason, *Development and application of micromechanical techniques for characterising interfacial shear strength in fibre-thermoplastic composites.* Polymer Testing, 2012. **31**(7): p. 895-903.

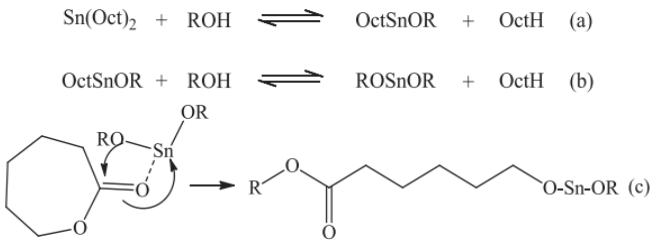

Figure 1: Initiation and propagation reactions for CIM polymerisation of ε-caprolactone

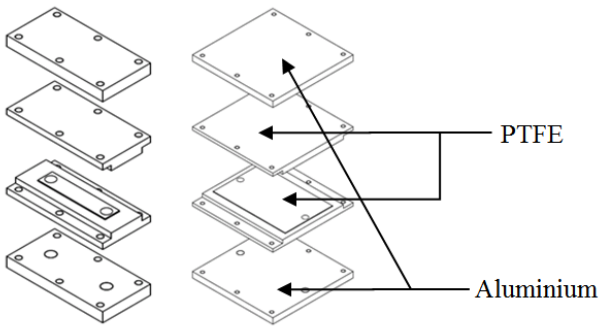

Figure 2: PTFE moulds for ISP

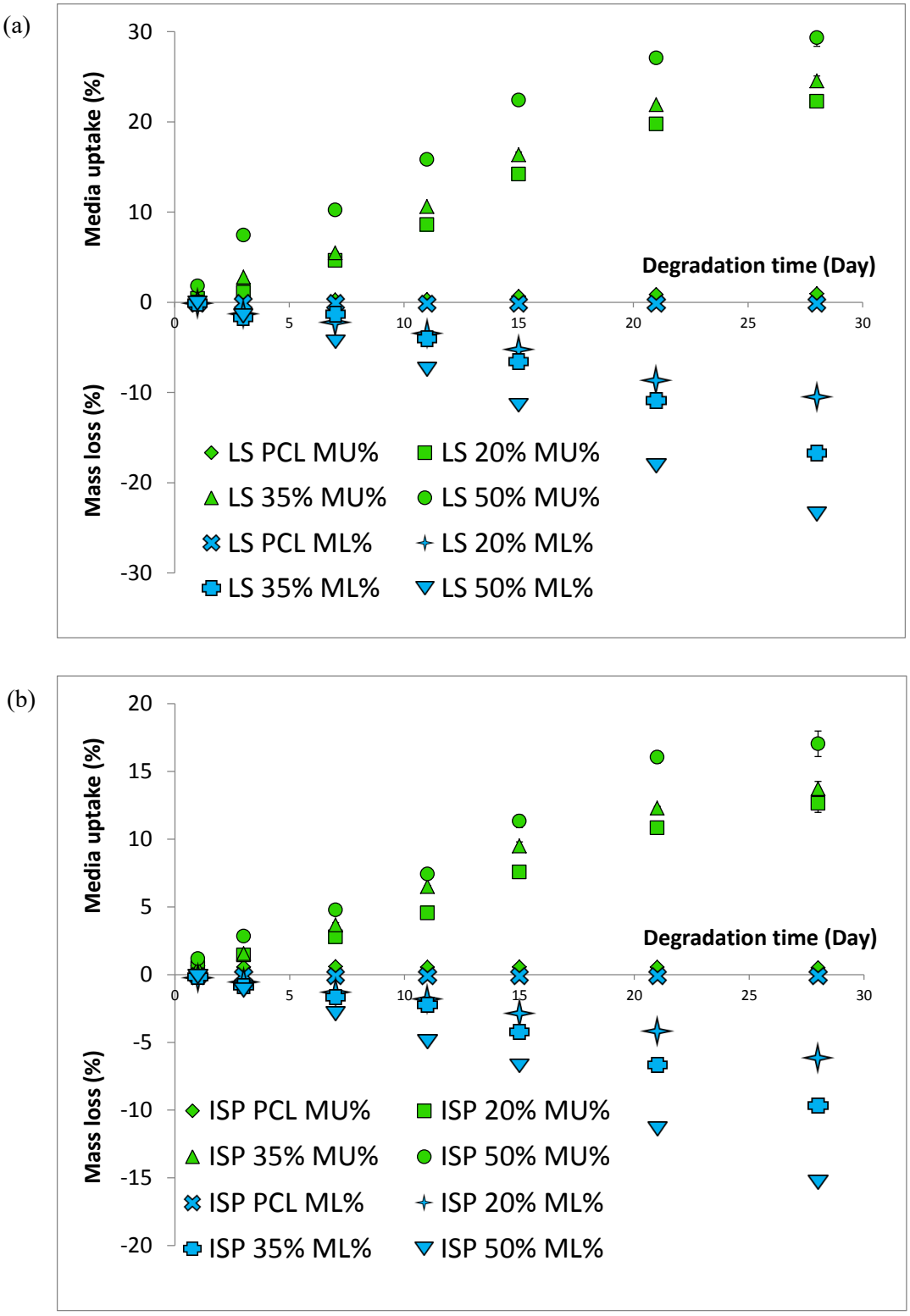

Figure 3: Variation of percentage media uptake and mass loss of the (a) LS PCL and PCL/PGF composites, (b) ISP PCL and PCL/PGF composites. Degradation study conducted in PBS at 37 °C.
LS = Laminate stacking, ISP = In-situ polymerisation, Fibre volume fraction = 20%, 35% and 50%.
MU% = % media uptake; ML% = % mass loss.

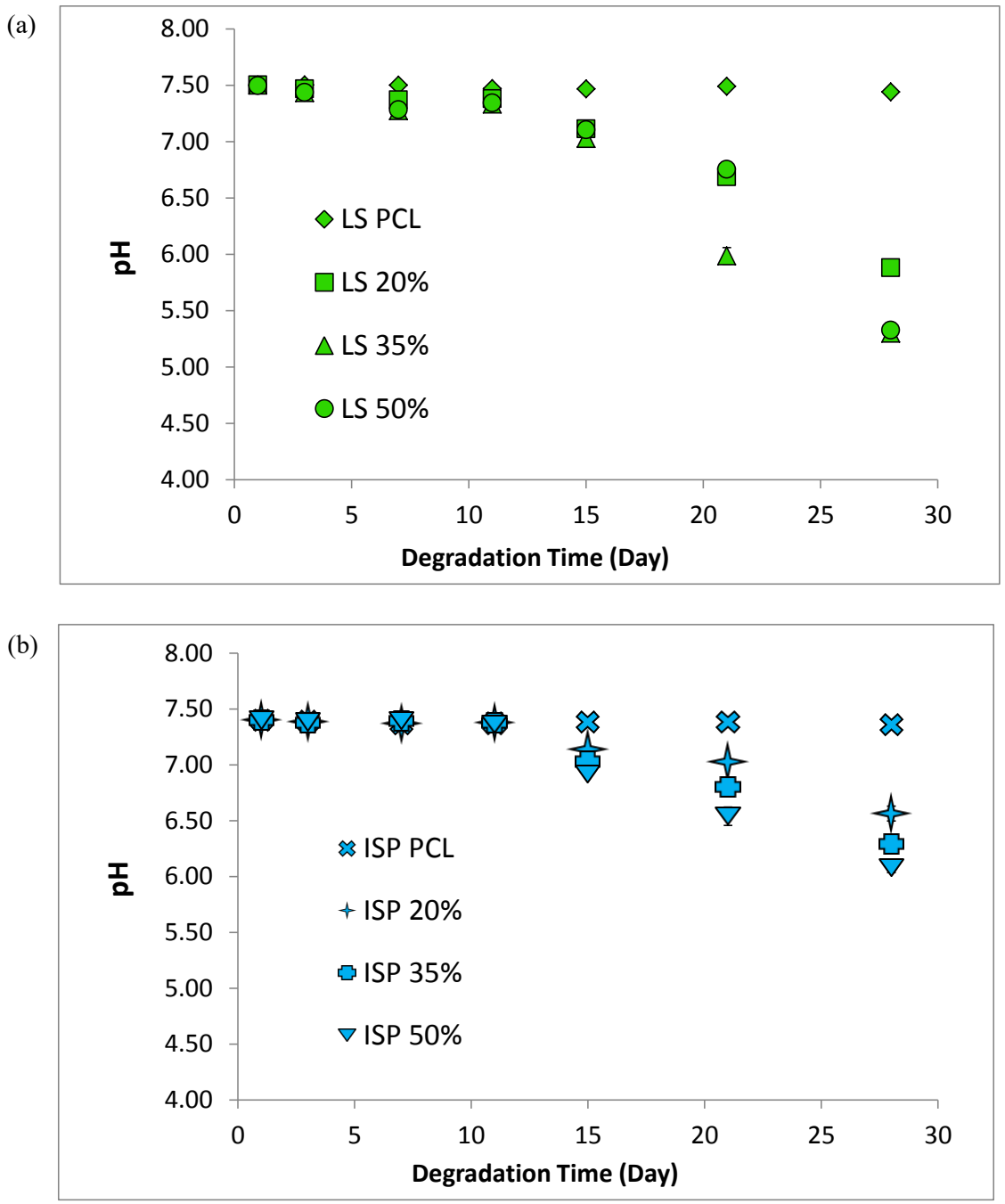

Figure 4: Variations in the pH values of PBS media during degradation for (a) Laminate stacked PCL and PCL/PGF composites, (b) In-situ polymerised PCL and PCL/PGF composites.
Degradation study conducted in PBS at 37 °C.
LS = Laminate stacking, ISP = In-situ polymerisation, Fibre volume fraction = 20%, 35%, 50%.

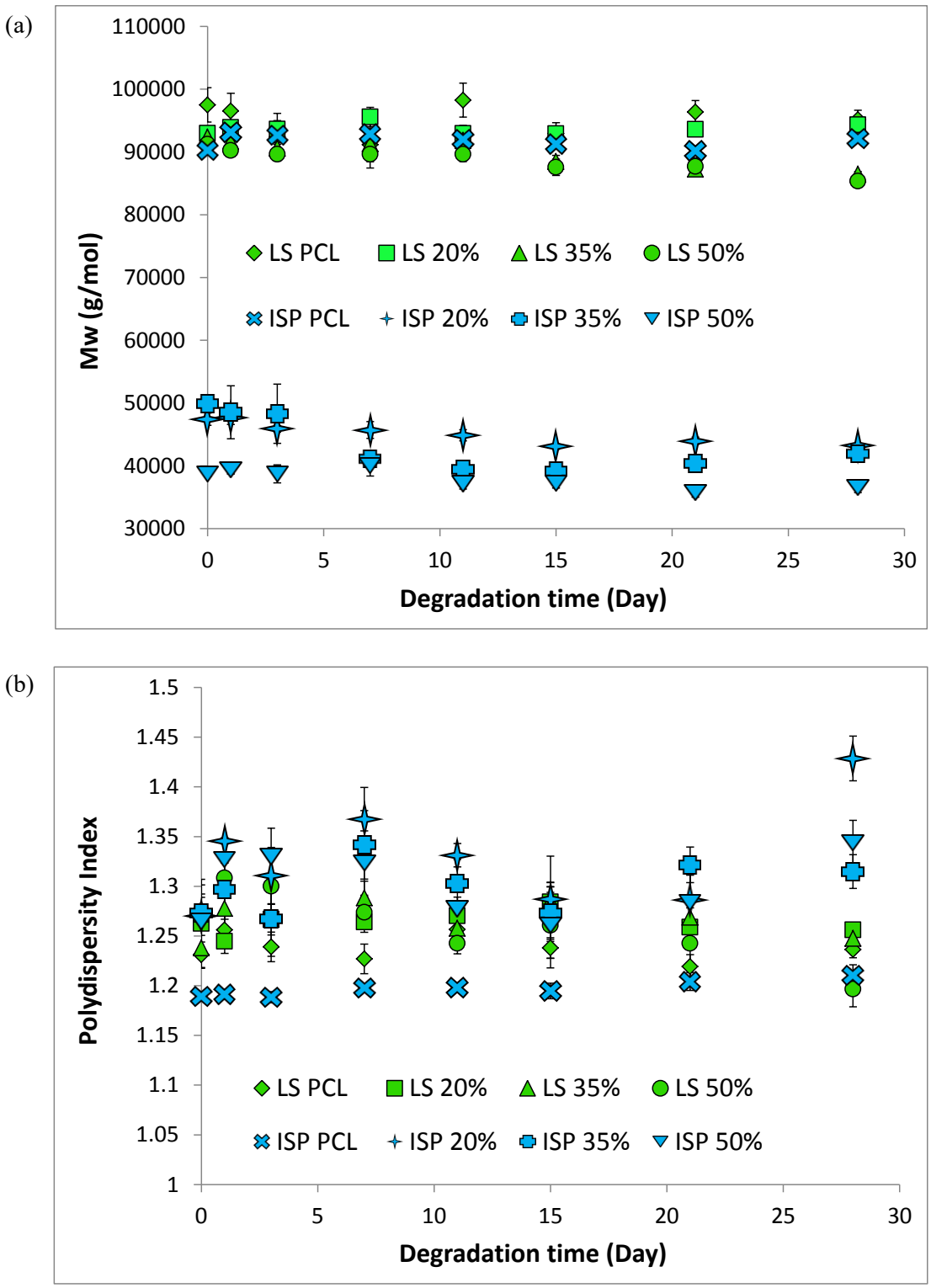

Figure 5: Variation of (a) Molecular weight (b) Polydispersity of LS and ISP PCL and PCL/PGF composites; Degradation study conducted in PBS at 37 °C. LS = Laminate stacking, ISP = In-situ polymerisation; Fibre volume fraction = 20%, 35% and 50%.

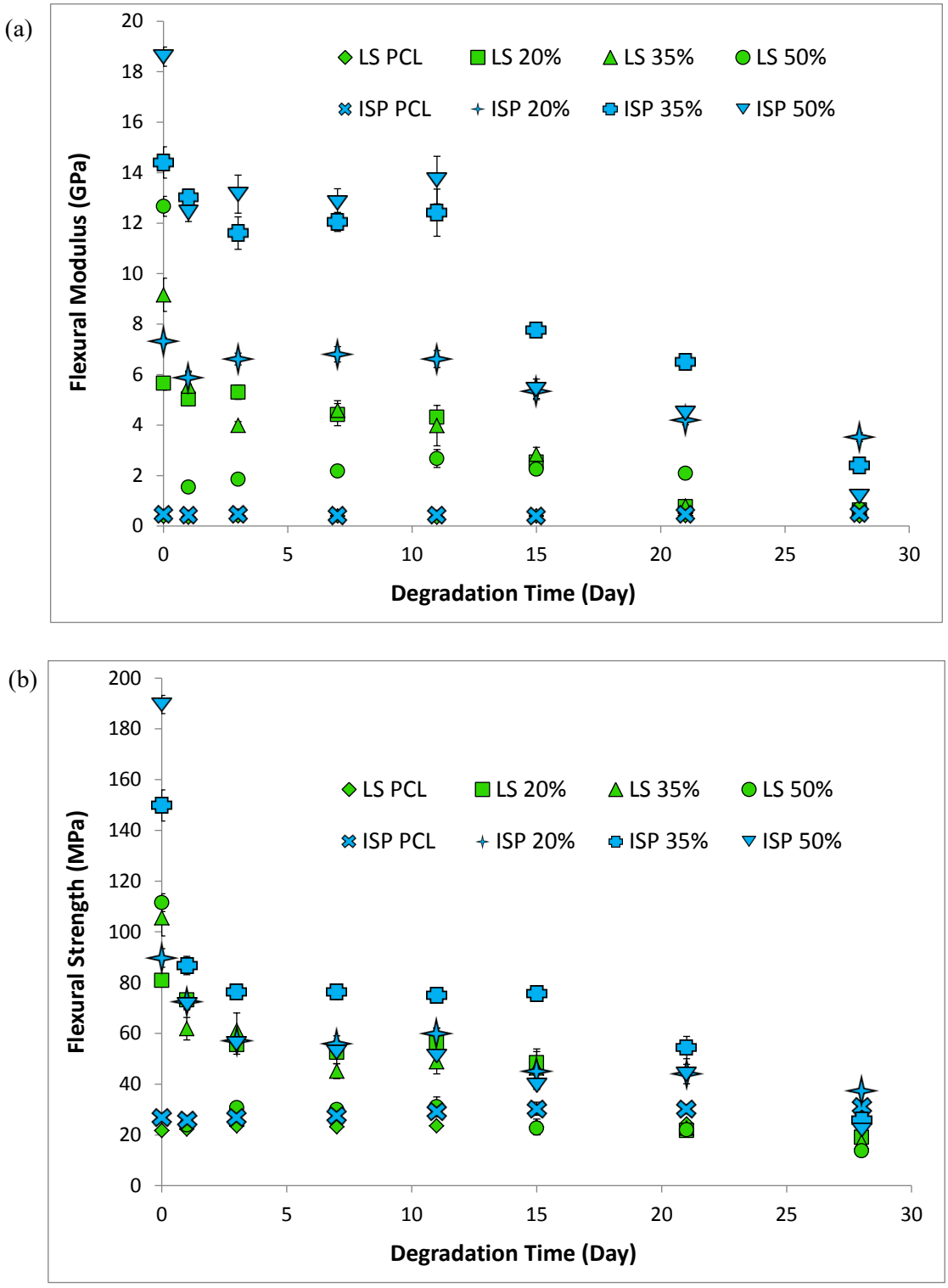

Figure 6: Variations of (a) flexural strength (b) flexural modulus of LS and ISP PCL and PCL/PGF composites; degradation study conducted in PBS at 37 °C for 28 days.
LS = Laminate stacking, ISP = In-situ polymerisation. Fibre volume fraction = 20%, 35% and 50%.

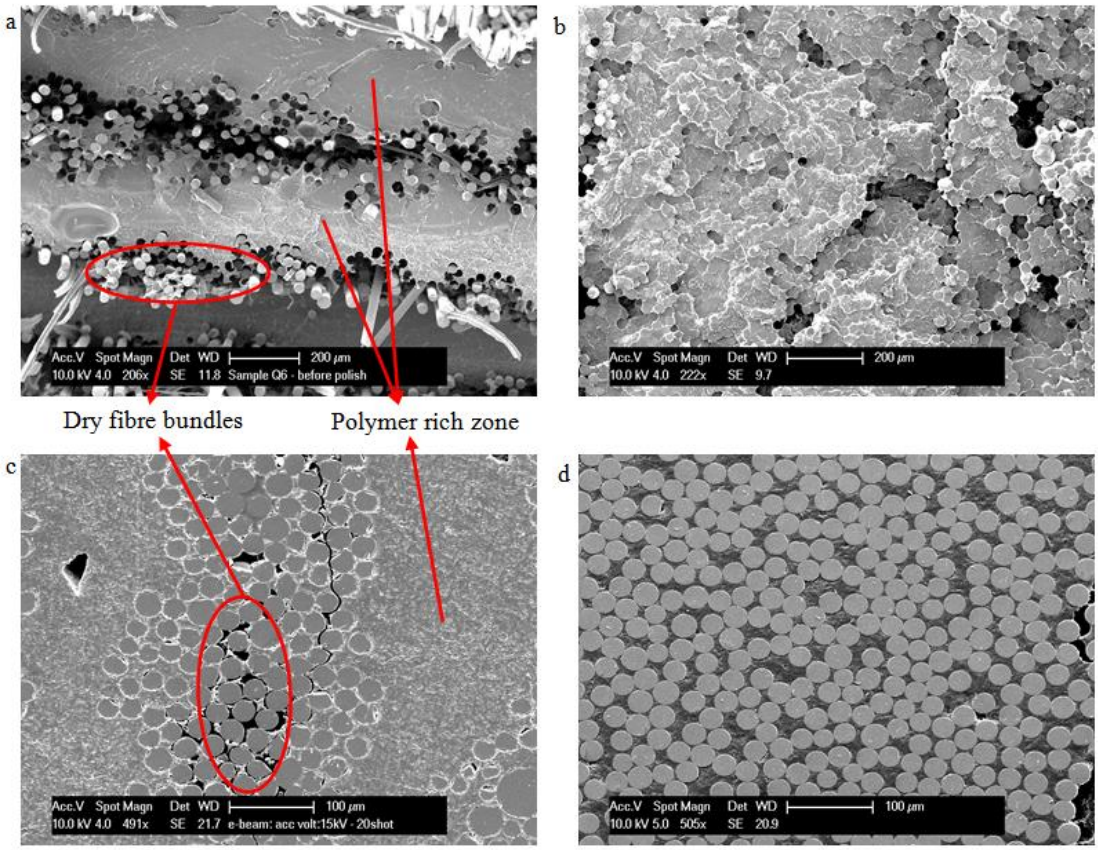

Figure 7: SEM micrographs of composites specimens before degradation: freeze fractured surface of (a) LS35, (b) ISP35; Cut polished surface of (c) LS35, (d) ISP35

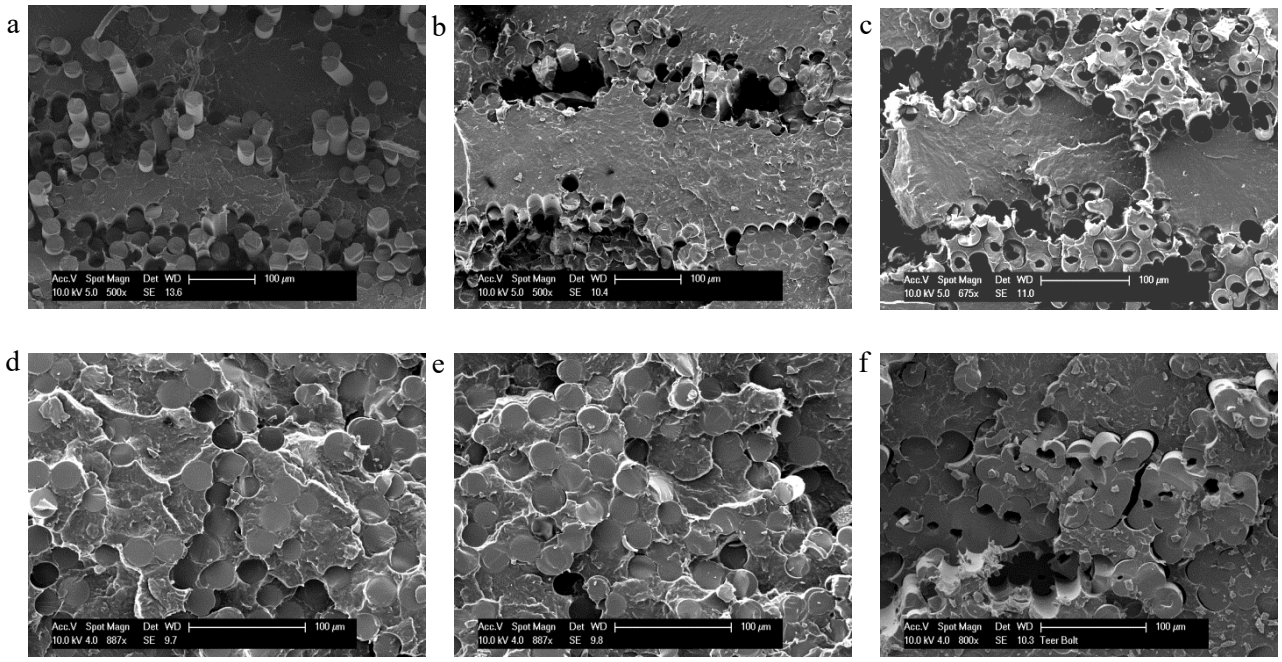

Figure 8: SEM micrographs of freeze fractured surfaces for LS35 samples post immersion in PBS at 37°C: (a) 1 day, (b) 15 days, (c) 28 days interval. In comparison ISP35 samples post immersion are shown (d) 1 day, (e) 15 days, (f) 28 days.

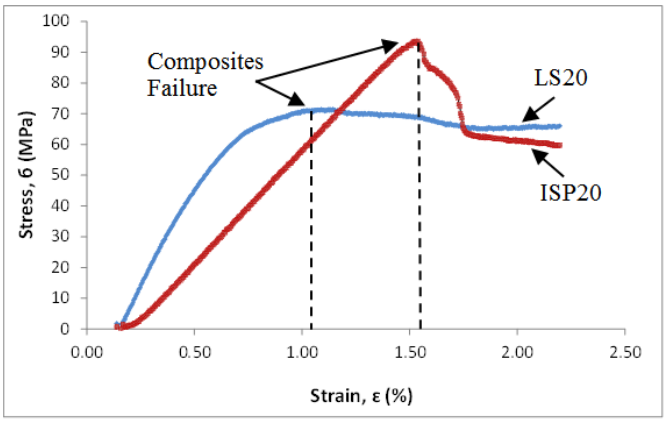

Figure 9: Stress strain curve of flexural tests for non-degraded LS20 and ISP20 composites

Table 1: Phosphate glass code and formulation

Glass code	P_2O_5 content (mol%)	CaO content (mol%)	Na_2O content (mol%)	MgO content (mol%)	Fe_2O_3 content (mol%)	Drying temp/time (°C/h)	Melting temp/time (°C/h)
P45Fe5	45	16	10	24	5	350/0.5	1100/1.5

Table 2: PCL/PGF composites volume fraction and codes

Manufacture technique	**Composite codes**	**Targeted V_f**	**Actual V_f**
Laminate Stacking (LS)	LSPCL	N/A	PCL only
	LS20	20%	3.0% ± 1.2%
	LS35	35%	29.1% ± 0.6%
	LS50	50%	49.0% ± 0.5%
In-situ Polymerisation (ISP)	ISPPCL	N/A	PCL only
	ISP20	20%	19.6% ± 2.1%
	ISP35	35%	31.5% ± 1.0%
	ISP50	50%	51.9% ± 1.8%

Table 3: Comparison between experimental and theoretical flexural modulus for LS and ISP composites

Sample code	**Experimental flexural modulus (GPa)**	**Theoretical flexural modulus range (GPa)**
LS20	5.6 ± 0.3	8.5 – 9.4
LS35	9.2 ± 0.7	10.9 – 11.3
LS50	12.7 ± 0.4	18.0 – 18.4
ISP20	7.3 ± 0.2	6.9 – 8.5
ISP35	14.4 ± 0.6	13.8 – 14.6
ISP50	18.6 ± 0.4	18.9 - 20.2